PHYSICAL REVIEW B **77**, 201405(R) (2008)

Large oscillating nonlocal voltage in multiterminal single-wall carbon nanotube devices

G. Gunnarsson, J. Trbovic, and C. Schönenberger
Department of Physics, University of Basel, Klingelbergstrasse 82, CH-4056 Basel, Switzerland
(Received 1 October 2007; revised manuscript received 24 March 2008; published 22 May 2008)

We report on the observation of a nonlocal voltage in a ballistic (quasi)-one-dimensional conductor, realized by a single-wall carbon nanotube with four contacts. The contacts divide the tube into three quantum dots, which we control by the back-gate voltage V_g. We measure a large *oscillating* nonlocal voltage V_{nl} as a function of V_g. Though a resistor model that includes the impedance of the voltmeter can account for a nonlocal voltage including change of sign, it fails to describe the magnitude properly. The large amplitude of V_{nl} is due to quantum interference effects and can be understood within the scattering approach of electron transport.

DOI: 10.1103/PhysRevB.77.201405 PACS number(s): 73.23.Ad, 73.63.Fg, 73.63.Nm

The recent realization of the spin field-effect transistor in carbon nanotube (CNT) devices[1] demonstrated the ability to control spin transport in a quantum dot (QD).[2] However, additional effects, such as the anomalous magnetoresistance, can contribute to the observed signal in spin valves.[3–6] It seems clear that despite a number of large responses seen in CNT-based devices,[1,7–9] one needs to go beyond two-terminal structures by realizing multi-terminal devices where nonlocal measurements are feasible.[10] The nonlocal measurement in spin-valve devices was pioneered by Johnson and Silsbee[11] in metallic spin valves and was further applied to various other systems.[12–14] This technique separates spin from charge effects by passing the current through the injection branch of the device and detecting the nonlocal voltage in the part of the device that does not lie in the charge current path. Recent application of the *nonlocal* spin technique in CNTs[10] showed the feasibility and yet tremendous challenge of performing such measurements in low-dimensional mesoscopic systems. The hallmark of these measurements is that a positive voltage is measured when the magnetization of the injector and detector electrodes is parallel, and a negative one *only* when they are antiparallel. However, it has been reported recently that the four-probe resistance with nonmagnetic probes in CNTs can be negative due to interference effects.[15] This suggests that the measurement of the *nonlocal* spin transport in mesoscopic systems such as CNTs with ferromagnetic contacts could be strongly influenced by quantum interference effects.

We report here on measurements of a large nonlocal voltage V_{nl} in multiterminal CNT devices [Fig. 1(a)] in the quantum dot (QD) regime, which changes sign and magnitude as the back-gate voltage is swept. We show that V_{nl} cannot be explained by a classical resistor model. Instead, a quantum approach is required. We also show that in these devices, which have relative transparent contacts with resistances in the range of 10–100 kΩ, the magnitude of the oscillating V_{nl} greatly exceeds any nonlocal spin signal.

Our devices consist of single-wall CNTs grown by chemical vapor deposition (CVD) and contacted with four probes as shown in Fig. 1(a). Two middle electrodes are ferromagnetic (F) made of PdNi(20 nm)/Co(25 nm)/Pd(10 nm) trilayer, whereas the two outer probes are normal (N) Pd(40 nm) electrodes. A PdNi alloy with 30% Pd is used, because it makes stable contacts to the CNT,[1] while Co serves as magnetization alignment layer for PdNi.[16] The device lies on a 400-nm-thick SiO_2 layer, with an underlying highly doped Si substrate that is used as a back gate. The CNT was localized with a scanning-electron microscope (SEM) and the structure was defined using electron-beam lithography.

Samples were cooled in a He4 cryostat to 1.8 K where the differential conductance ($G=dI/dV_0$) was measured using standard low-frequency lock-in technique with an excitation voltage of $V_0=100$ μV. Two-terminal local G measurements were made across the three segments of the sample [schematics in Fig. 1(c)] in the gate voltage range $V_g=1.4-2.4$ V, see Figs. 2(a)–2(c). G is found in the range of $0.1-2e^2/h$ and strongly varies as a function of V_g, as expected for a QD. By sweeping a dc source-drain voltage V_{sd}, we have obtained a gray-scale plot of G for the right segment 3-4 [inset of Fig. 2(c)]. The conductances of the three segments display qualitatively similar patterns in different V_g ranges, but the fine structure may vary. This particular V_g range has been selected for Fig. 2, because of the pronounced fourfold pattern[17,18] in the voltage detection arm of the nonlocal measurement, proving the absence of

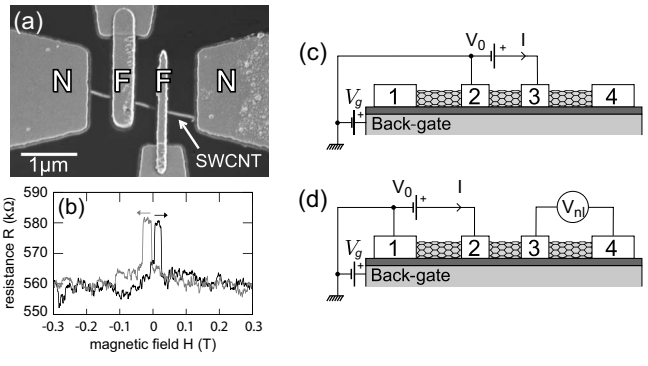

FIG. 1. (a) A SEM image of a device. The metallic single-wall CNT is contacted with two ferromagnetic (F) and two normal contacts (N), which together divide the tube into three equidistant segments ($L\approx 500$ nm) which act as QDs. (b) Two-terminal magnetoresistance signal (F-F). (c,d) Schematics of the measurement setup for the local two-terminal (c) and nonlocal four-terminal (d) measurement.

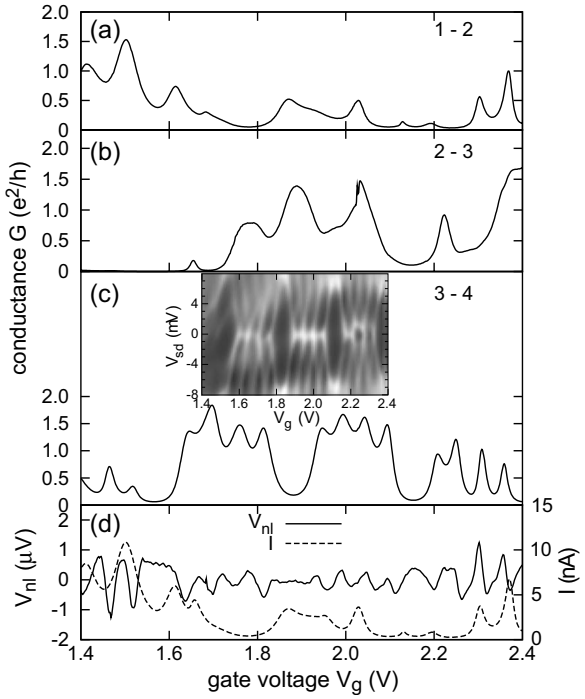

FIG. 2. (a)–(c) Linear conductance G of each segment of the device as a function of gate voltage V_g. The inset of (c) shows a gray-scale plot of dI/dV_0 as function of V_g and source-drain bias V_{sd} in the same V_g range. (d) Nonlocal voltage measured across terminals 3 and 4 (full curve) and the current injected across terminals 1 and 2 (dashed).

intratube scattering, and the presence of a QD formed by an *individual* single-wall CNT.

The nonlocal voltage measured across segment 3-4 is shown in Fig. 2(d) (full) together with the current I (dashed curve) injected through segment 1-2 and driven by a constant ac voltage V_0 of 200 μV. Two very striking features are noticeable in these measurements. First, the nonlocal voltage V_{nl} oscillates around zero, and secondly, the amplitude is large with a typical value of 1 μV. This results in an oscillating nonlocal resistance $R_{nl}=V_{nl}/I$ with values of 0.1–1 kΩ. A similar behavior is found in different gate-voltage ranges, as well as in different samples; see, e.g., Fig. 3.

In order to understand the origin of the observed signal, we first model our device as a classical network of resistors, shown in Fig. 4(a).[10] Each terminal in the circuit is characterized by contact resistances R_{ci} and r_{ci}, and the CNT sections between terminals i and its next neighbors j have resistances R_{ij}. Two limiting cases are shown in (b) and (c) of Fig. 4: in case (b) of "noninvasive" contacts ($R_c \gg r_c$), all contacts 1-4 couple weakly to the CNT. In contrast, in case (c) of "strongly invasive" contacts ($R_c \ll r_c$), the CNT is split into segments. Although there have been reports on both strong and weak contacts to CNTs,[19] a typical device lies in between. For weak contacts [Fig. 4(b)], driving a current in the left branch results in the appearance of a *uniform* voltage V' on the CNT. Hence, $V_3=V_4=V'$ and the nonlocal voltage $V_{nl}:=V_3-V_4=0$. For strong contacts [Fig. 4(c)], V_3 and V_4 equal the bias voltage V_0, leading again to a vanishing nonlocal voltage. Because we have assumed ideal voltage probes in which no current flows, the right arm must have a uniform potential also in the general case. We therefore conclude that $V_{nl}=0$ in the classical limit. This breaks down, if the elctrometers are not ideal, but possesses a finite input impedance, thereby providing a current sink.

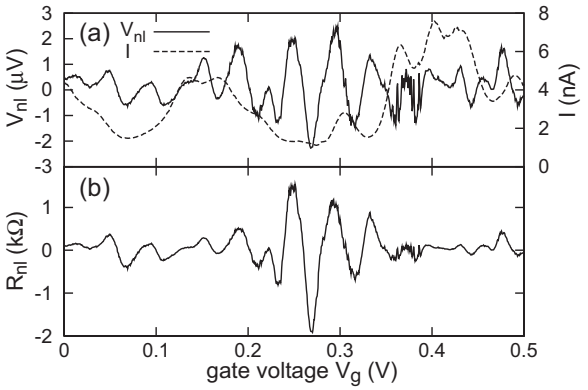

FIG. 3. Nonlocal measurement as a function of gate voltage V_g of another device. (a) The current I between terminals 1-2 (dashed) is plotted together with the nonlocal voltage V_{nl} between terminals 3-4 (solid). (b) Calculated nonlocal resistance $R=V_{nl}/I$.

We next take the input amplifier input impedances $R_I=100$ MΩ, appearing at the voltage probes 3 and 4, in the resistor model in Fig. 4(a) into account. Assuming a ballistic wire with $R_{ij}=0$, we obtain the following for V_{nl} of the third segment (3-4): $V_{nl}\approx V_2^*(r_{c3}+r_{c4}+R_{c4}-R_{c3})/R_I$, where V_2^* is the potential at the inner node of contact 2, as shown in Fig.

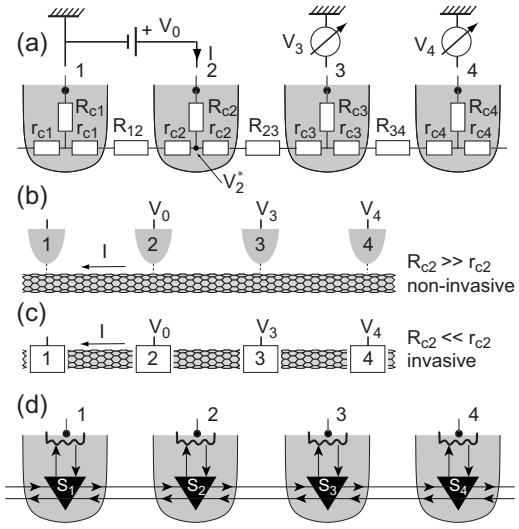

FIG. 4. (a) Resistor model for metal-CNT contacts. The three resistors in each shaded region model the property of the contact, whereas R_{34}, for example, describes the intratube resistance in between contacts 3 and 4. Two limiting cases are shown in (b) and (c): In (b), the contacts are weakly coupled to the CNT, whereas they split the CNT into segments due to their strong coupling in (c). (d) shows the quantum description, using three-port scattering matrices S_j (triangles) in each node. Note that there is an additional input resistance R_I (not shown) in both electrometers measuring V_3 and V_4.

4(a). V_2^* is of order V_0. that because of the minus sign in one term, a negative V_{nl} is possible for certain resistance values. If the magnitude of all contact resistances is similar, however, a positive "mean" nonlocal voltage is predicted, in disagreement with the experiment. The observation of an oscillating V_{nl} with a mean value close to zero could only be reconciled with the classical model if $r_c \ll R_c$. Then, the equation simplifies and we arrive at the following estimate: $V_{nl} \approx V_0(R_{c4}-R_{c3})/R_I$.This formula predicts that V_{nl} follows the gate-voltage behavior of the resistances of contact 3 and 4. Using a typical contact resistance for our device of 100 kΩ, $R_I=100$ MΩ, and $V_0=200$ μV, we estimate $V_{nl} \sim 0.2$ μV. This is an order of magnitude smaller than measured in the experiment, where the oscillating nonlocal voltage peaks up to $V_{nl} \sim 2$ μV. In order to be absolutely certain that the current in the detector arm caused by the finite input impedance R_I of the amplifiers is not the source of V_{nl}, we have crossed-checked these measurements with a custom-modified amplifier with an input impedance of $R_I=1$ GΩ and have found no change in V_{nl}. We are therefore confident that the classical resistor model cannot account for the measured oscillating nonlocal voltage V_{nl} and that the finite input impedance of the amplifiers is not the source of this signal.

To understand the magnitude of the nonlocal voltage, we next move on to a quantum-coherent description. We apply the scattering approach[20] to calculate V_{nl}. A similar approach was taken by Lerescu *et al.*, but for an open cavity that supports many modes.[21] In contrast, in our case of a CNT we deal with a (quasi)-one-dimensional (1D) system. This approach is sketched in Fig. 4(d). The triangles in each node j denote a three-port scattering matrix S_j. If we assume that each port is described by a one-mode conductor, S_j is a 6×6 matrix that describes the amplitudes between outgoing and incoming waves.[20] If we stick to a one-mode conductor, one can prove that $V_{nl}=0$, independent of any details of S_j. This theorem of vanishing nonlocal voltage in a 1D conductor can be traced back to the particular structure of the whole S matrix in which the S_j's are connected *in series*. Hence, similar to the resistor model, even in the coherent description, the nonlocal voltage is expected to disappear, provided the wire is 1D. Because we do measure a large V_{nl} in our devices, one of the assumptions in the theorem must be violated. These are as follows: linear response and truly 1D. For the former, we note that the maximum applied voltage of 200 μV corresponds to 2.3 K,which is slightly above the measurement temperature. But we have also measured at 100 μV and below confirming linearity. For the latter, we emphasize that V_{nl} does not change with the relative magnetization direction of the two ferromagnetic contacts, so that the spin degeneracy is not lifted. What remains as an explanation is the fact that due to the so-called K and K' degeneracy of graphene,[22] any CNT should carry two (orbitally) degenerate 1D modes. This then leads to the well-known fourfold pattern[17,18] in the spectrum of a CNT-QD, which is clearly visible in Fig. 2(c).

In order to estimate V_{nl}, we use the Landauer-Büttiker formalism.[20] The current I_i in lead i is given by $I_i \propto (N-R_i)V_i - \Sigma T_{ij}V_j$, where N denotes the number of modes (here $N=2$), R_i is the total reflection coefficient for contact i,

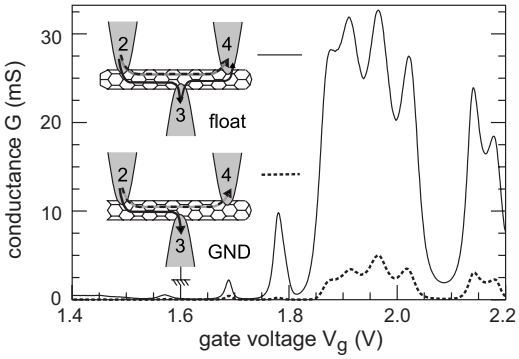

FIG. 5. Measurements of the two-terminal conductance G_{42} between terminals 2 and 4 while terminal 3 is floating (line) and while it is grounded (dashed line). The inset depicts transmission through the CNT in both cases.

T_{ij} is the probability that a charge carrier is transmitted from contact j to contact i, and V_k is the potential at contact k. Using this formalism, one can derive a compact formula for a general four-terminal voltage.[20] For our geometry, one obtains $V_{nl}=V_0(T_{32}T_{41}-T_{42}T_{31})/D$, where the denominator D is given by $D=(N-R_4)(N-R_3)-T_{34}T_{43}$. This expression can only be evaluated (estimated) if we can, in addition to nearest-neighbor transmissions, estimate the transmission probabilities that embrace second- or even third-nearest-neighbor contacts. These are the coefficients T_{31}, T_{42}, and T_{41}. For the former two, the electron wave has to be able to transmit *under* one contact (2 or 3) without relaxation, while for the latter even both contacts 2 and 3 need to be passed. We estimate this transmission beneath a contact by comparing the conductance G_{42} between terminals 2 and 4 when contact 3 is floating or grounded. The result is shown in Fig. 5. If the intermediate contact is floating, electrons that are transmitted into contact 3 must be reinjected into the device so that the transmission between 2 and 4 can be large. On the other hand, for rather strong-coupling contacts such as ours, only a small fraction of electrons is expected to transmit unperturbed under the contact. If contact 3 is now grounded, most carriers disappear via contact 3 to ground. This latter situation is indeed realized as shown in the data of Fig. 5. The dashed curve is suppressed by approximately a factor of 7–8. Hence, a fraction of 13% can pass under the contact by direct transmission.[23] This is surprisingly large given the typical values of the two-terminal resistances and the fact that the metal electrodes were evaporated directly onto a freshly CVD-grown CNT. Let us assume that transmission under the contact is similar for contacts 2 and 3 and let us denote this probability by t. The magnitude of V_{nl}/V_0 is then estimated by t^2, so that $|V_{nl}| \lesssim 3.5$ μV, in good agreement with the measured V_{nl}.

We now turn our attention to spin transport and estimate the expected spin-dependent nonlocal voltage V_{nl}^{spin}. We use the resistor model shown in Fig. 4(a). This time, however, one has to expand it by introducing separate spin-up and spin-down channels. The contact resistances at F contacts depend on the relative orientation of the electron spin and the magnetization within the F contacts.[10] For simplicity, we assume that different contacts have equal resistances. We em-

phasize here that for the detection of a nonlocal spin signal, the spin imbalance in the injector part 1-2 has to be able to "diffuse" into the detector branch. In the strongly invasive limit this is impossible, because the strongly coupled contact 2 would equilibrate the spin imbalance. In contrast, for weakly coupling contacts, a spin imbalance in the CNT caused by spin injection can be sensed by an F contact. $V_{\mathrm{nl}}^{\mathrm{spin}}$, therefore, strongly depends on the ratio $r:=r_c/R_c$. Assuming a small contact polarization p, one obtains $V_{\mathrm{nl}}^{\mathrm{spin}}/V_0=p^2\times 0.25$ if $r\ll 1$, which is the largest possible signal. Using the measurement shown in Fig. 5, we can estimate the r ratio for our devices. We obtain $r\simeq 6$. This then yields $V_{\mathrm{nl}}^{\mathrm{spin}}/V_0\simeq p^2\times 0.0037$. We estimate p from the typical two-terminal TMR of $\approx 4\%$,[1,24,25] yielding a polarization of $\approx 20\%$. Inserting p and $V_0=200\ \mu\mathrm{V}$, the expected spin-dependent nonlocal voltage is only $V_{\mathrm{nl}}^{\mathrm{spin}}\simeq 30$ nV, two orders of magnitude smaller than the measured nonlocal voltage.

In conclusion, we find large oscillating nonlocal signals in all of our CNT quantum dot devices. The existence of such a background, which changes its sign with the back-gate voltage, can screen the nonlocal signals due to spin in particular in devices with relative high contact transparency.

Note added. Recently, we have become aware of a similar, but independent study by A. Makarovski *et al.*.[23]

Support by the Swiss NSF, the NCCR on Nanoscale Science, and EU-FP6-IST project HYSWITCH is gratefully acknowledged. Fruitful discussions with B. J. van Wees are gratefully acknowledged.

[1] S. Sahoo, T. Kontos, J. Furer, C. Hoffmann, M. Gräber, A. Cottet, and C. Schönenberger, Nat. Phys. **1**, 99 (2005).
[2] S. J. Tans, M. H. Devoret, H. Dai, A. Thess, R. E. Smalley, L. J. Geerligs, and C. Dekker, Nature **386**, 474 (1997); M. Bockrath, D. H. Cobden, P. L. McEuen, N. G. Chopra, A. Zettl, A. Thess, and R. E. Smalley, Science **275**, 1922 (1997); D. H. Cobden, M. Bockrath, P. L. McEuen, A. G. Rinzler, and R. E. Smalley, Phys. Rev. Lett. **81**, 681 (1998).
[3] See, for example, H. X. Tang, F. G. Monzon, M. L. Roukes, F. J. Jedema, A. T. Filip, and B. J. van Wees, in *Semiconductor Spintronics and Quantum Computation*, edited by D. D. Awschalom, N. Samarth, and D. Loss (Springer-Verlag, Berlin, 2002).
[4] H. X. Tang, R. K. Kawakami, D. D. Awschalom, and M. L. Roukes, Phys. Rev. Lett. **90**, 107201 (2003).
[5] C. Gould, C. Rüster, T. Jungwirth, E. Girgis, G. M. Schott, R. Giraud, K. Brunner, G. Schmidt, and L. W. Molenkamp, Phys. Rev. Lett. **93**, 117203 (2004).
[6] S. J. van der Molen, N. Tombros, and B. J. van Wees, Phys. Rev. B **73**, 220406(R) (2006).
[7] H. T. Man, I. J. W. Wever, and A. F. Morpurgo, Phys. Rev. B **73**, 241401(R) (2006).
[8] B. Zhao, I. Mönch, H. Vinzelberg, T. Mühl, and C. M. Schneider, Appl. Phys. Lett. **80**, 3144 (2002).
[9] L. E. Hueso, J. M. Pruneda, V. Ferrari, G. Burnell, J. P. Valdes-Herrera, B. D. Simons, P. B. Littlewood, E. Artacho, A. Fert, and N. D. Mathur, Nature **445**, 410 (2007).
[10] N. Tombros, S. J. van der Molen, and B. J. van Wees, Phys. Rev. B **73**, 233403 (2006).
[11] M. Johnson and R. H. Silsbee, Phys. Rev. Lett. **55**, 1790 (1985).
[12] F. J. Jedema, A. T. Filip, and B. J. van Wees, Nature **410**, 345 (2001).
[13] X. Lou, C. Adelmann, S. A. Crooker, E. S. Garlid, J. Zhang, K. S. M. Reddy, S. D. Flexner, C. J. Palmstrom, and P. A. Crowell, Nat. Phys. **3**, 197 (2007).
[14] N. Tombros, C. Jozsa, M. Popinciuc, H. T. Jonkman, and B. J. van Wees, Nature **448**, 571 (2007).
[15] B. Gao, Y. F. Chen, M. S. Fuhrer, D. C. Glattli, and A. Bachtold, Phys. Rev. Lett. **95**, 196802 (2005).
[16] Detailed measurements of the magnetic properties of a PdNi/Co bilayer will be published elsewhere.
[17] W. Liang, M. Bockrath, and H. Park, Phys. Rev. Lett. **88**, 126801 (2002).
[18] M. R. Buitelaar, A. Bachtold, T. Nussbaumer, M. Iqbal, and C. Schönenberger, Phys. Rev. Lett. **88**, 156801 (2002).
[19] See for example, M. Bockrath, D. H. Cobden, L. Jia, A. G. Rinzler, R. E. Smalley, L. Balents, and P. L. McEuen, Nature **397**, 598 (1999); A. Bachtold, M. de Jonge, K. Grove-Rasmussen, P. L. McEuen, M. Buitelaar, and C. Schönenberger, Phys. Rev. Lett. **87**, 166801 (2001).
[20] M. Büttiker, Phys. Rev. Lett. **57**, 1761 (1986).
[21] A. I. Lerescu, E. J. Koop, C. H. van der Wal, B. J. van Wees, and J. H. Bardarson, arXiv:0705.3179v1.
[22] M. S. Dresselhaus, G. Dresselhaus, and P. C. Eklund, *Science of Fullerenes and Carbon Nanotubes* (Academic, New York, 1996).
[23] A. Makarovski, A. Zhukov, J. Liu, and G. Finkelstein, Phys. Rev. B **76**, 161405(R) (2007).
[24] M. Jullière, Phys. Lett. **54A**, 225 (1975).
[25] I. Zutic, J. Fabian, and S. Das Sarma, Rev. Mod. Phys. **76**, 323 (2004).